ORIGINAL ARTICLE

Open Access

Piper betle-mediated green synthesis of biocompatible gold nanoparticles

Jayasekhar Babu Punuri[1,2], Pragya Sharma[2], Saranya Sibyala[2,3], Ranjan Tamuli[2] and Utpal Bora[1,2*]

Abstract

Here, we report the novel use of the ethonolic leaf extract of *Piper betle* for gold nanoparticle (AuNP) synthesis. The successful formation of AuNPs was confirmed by UV-visible spectroscopy, and different parameters such as leaf extract concentration (2%), gold salt concentration (0.5 mM), and time (18 s) were optimized. The synthesized AuNPs were characterized with different biophysical techniques such as transmission electron microscopy (TEM), Fourier transform infrared (FT-IR) spectroscopy, X-ray diffraction (XRD), and energy-dispersive X-ray spectroscopy (EDX). TEM experiments showed that nanoparticles were of various shapes and sizes ranging from 10 to 35 nm. FT-IR spectroscopy revealed that AuNPs were functionalized with biomolecules that have primary amine group $-NH_2$, carbonyl group, $-OH$ groups, and other stabilizing functional groups. EDX showed the presence of the elements on the surface of the AuNPs. FT-IR and EDX together confirmed the presence of biomolecules bounded on the AuNPs. Cytotoxicity of the AuNPs was tested on HeLa and MCF-7 cancer cell lines, and they were found to be nontoxic, indicating their biocompatibility. Thus, synthesized AuNPs have potential for use in various biomedical applications.

Keywords: Nanocrystalline materials, Biomaterials, Crystal growth, Electron microscopy, Fourier transform infrared spectroscopy, Biosynthesis, Nucleation

Background

Synthesis of gold nanoparticles (AuNPs) has gained immense significance during the last few years due to their catalytic, optical, and electrical properties [1]. The existing chemical and physical methods are successful in producing well-defined AuNPs, but these processes usually require use of toxic chemicals. Therefore, the synthesized nanoparticles are not useful in medical and biological applications [2-4]. For this reason, the synthesis of AuNPs using an eco-friendly method is important to address the growing concerns on the overall toxicity of nanoparticles for medical and biotechnological applications. AuNPs have been considered important due to their unique and tunable surface plasmon resonance (SPR) property and their applications in biomedical science including drug delivery, tissue/tumor imaging,

photo thermal therapy, immune chromatography, and identification of pathogens in clinical specimens [5]. It is known that the physico-chemical properties of AuNPs are strongly dependent upon their interaction with capping agent molecules [6]. Indeed, the surface chemistry of AuNPs can modify their interaction with external systems [7]. This study describes an eco-friendly method for the synthesis of AuNPs using *Piper betle* as the reducing and stabilizing agent.

P. betle Linn (family: Piperaceae) leaves are widely used as a post-meal mouth freshener, and the crop is extensively grown in India, Sri Lanka, Malaysia, Thailand, Taiwan, and other Southeast Asian countries. The leaves of this plant are economically and medicinally important and have been traditionally used in India, China. In Thailand leaves are used to prevent oral malodor since it has an antibacterial activity against obligate oral anaerobes responsible for halitosis [8]. Aqueous extracts of *P. betle* have also been shown to reduce the adherence of early dental plaque bacteria [9]. The leaves of *P. betle* have a strong pungent and aromatic flavor and are used as a mouth freshener, in wound healing [10], as a digestive and

---

* Correspondence: Ubora@rediffmail.com
[1]Biomaterials and Tissue Engineering Laboratory, Department of Biotechnology, Indian Institute of Technology Guwahati, Guwahati, Assam 781039, India
[2]Biotech Hub, Centre for the Environment, Indian Institute of Technology Guwahati, Guwahati, Assam 781039, India
Full list of author information is available at the end of the article

pancreatic lipase stimulant [11], antioxidant [12,13], antifungal, antibacterial [1,14-16], anti-inflammatory, bioprotective [17], and antidiabetic [18] agent. In Chinese folk medicine, it is used for curing wind-cold cough, bronchial asthma, rheumatism, stomachalgia, and pregnancy edema [19]. *P. betel* leaves contain a significant amount of antioxidants such as hydroxychavicol, eugenol, ascorbic acid, and β-carotene [20]. We have successfully synthesized AuNPs by hypothesizing that the presence of strong antioxidants and flavonoids would assist in the reduction of gold ions to AuNPs. To aid this process, we applied microwave (MW) irradiation, which has the advantages of homogeneous heating that directly influence the nucleation process of AuNPs synthesis [21,22]. Cytotoxicity tests were done to examine the effect of the synthesized AuNPs on the proliferation of two human cancer cell lines and revealed that the synthesized AuNPs were biocompatible. Therefore, AuNPs synthesized using this method can potentially be used in biomedical applications.

Methods
Materials
P. betel was collected from a local market in Guwahati, India. The reagents were of analytical grade obtained either from Merck (Mumbai, India) or Sisco Research Laboratories (Mumbai, India). 3,4,5-Dimethylthiazol-2-yl-2-5-diphenyltetrazolium bromide (MTT) was purchased from Hi Media (Bangalore, India). Cell lines were obtained from the National Centre for Cell Sciences (Pune, India). Cell culture-related plasticware were obtained from Sigma-Aldrich (Bangalore, India).

Preparation of leaf extract
P. betel leaves were washed with deionized water to remove adsorbed dirt. The leaves were chopped into small pieces (2×2 cm) and dried at room temperature (25°C) under shade. The dried leaves were powered in a mixer grinder (Bajaj Model GX 11, Mumbai, India). Five grams of powder was dissolved in 50 ml of ethanol and kept at 4°C for 1 week to get the leaf extract. The *P. betle* leaf extract (PLE) was filtered using a Whatman (50 mm; Sigma, Bangalore, India) filter paper, and the filtrate was stored at 4°C for various experiments.

Synthesis of AuNPs
The synthesis of AuNPs was carried out by varying the PLE concentration (0.5% to 4%) against 0.5 mM $HAuCl_4$ in a total volume of 2 ml made up with double distilled water. The resulting mixtures were placed in a domestic microwave oven (900 W, 2.45 GHz, LG MO- MC-767 W/WS, LG Corp., Noida, India) and irradiated for 15 s. To obtain the optimum concentration of $HAuCl_4$, the experiments were carried out by varying the gold

solution concentration against 2% of PLE. The optimum time for synthesis was determined by incubating 2% of PLE with 0.5 mM by varying the MW irradiation time from 12 to 30 s with an interval of 2 s.

Characterization of AuNPs
UV-visible spectroscopy
All UV-visible (UV–vis) spectroscopic measurements of the synthesized AuNPs were carried out on a Cary 100 BIO UV–vis spectrophotometer (Varian, Palo Alto, CA, USA).

Transmission electron microscope
Colloidal solution (5 ml) of synthesized AuNPs was centrifuged twice at 20,000 rpm for 20 min to remove the non-covalently bounded molecules on the their surfaces. The resulting pellet was redispersed in 1 ml of distilled water, a few drops were placed over a carbon-coated copper grid, and the water was evaporated in a hot air oven (Daihan Labtech Co.Ltd. model LDO-150 F, New Delhi, India) at 60°C for 4 h. Transmission electron microscope (TEM) measurements were performed on a TEM instrument (JEOL model 2100, JEOL Ltd., Tokyo, Japan) operated at 190 V of 200 kV.

XRD, FT-IR, and EDX analyses
To obtain the X-ray diffraction (XRD) pattern, AuNP solution was placed on a microscope glass slide and allowed to dry in a hot air oven at 50°C, and the process was repeated to form a layer on the glass slide. The dried samples were analyzed with the help of an XRD instrument (Bruker Advance D8 XRD machine, Bruker, Madison, WI, USA) with a Cu source at 1.5406 Å wavelength in thin film mode.

AuNP colloidal solution (50 ml) was synthesized with optimum parameters (2% of PLE, 0.5 mM HAuCl, and 18 s) and centrifuged at 20,000 rpm for 20 min, and the process was repeated twice to remove non-covalently bounded molecules. The resulting pellet was resuspended in 5 ml of distilled water and lyophilized (Christ Gefriertrocknungsanlagen GmbH Model 1–4, Osterode, Germany) for 16 h. Infrared spectra were recorded using a Fourier transform infrared (FT-IR) spectroscope (Spectrum One, Perkin Elmer, Waltham, MA, USA) from 4,000/cm to 450/cm, with a resolution of 2 cm and five scans/sample by using 1 mg of finely powdered AuNPs prepared with 200 mg of KBr.

The elemental composition of the AuNPs was obtained by using energy-dispersive X-ray spectroscopy (EDX; LEO 1430 VP, Carl Zeiss AG, Oberkochen, Germany) at variable pressure and a scanning electron microscope equipped with INCA Oxford EDX facility at an acceleration voltage of 10 keV.
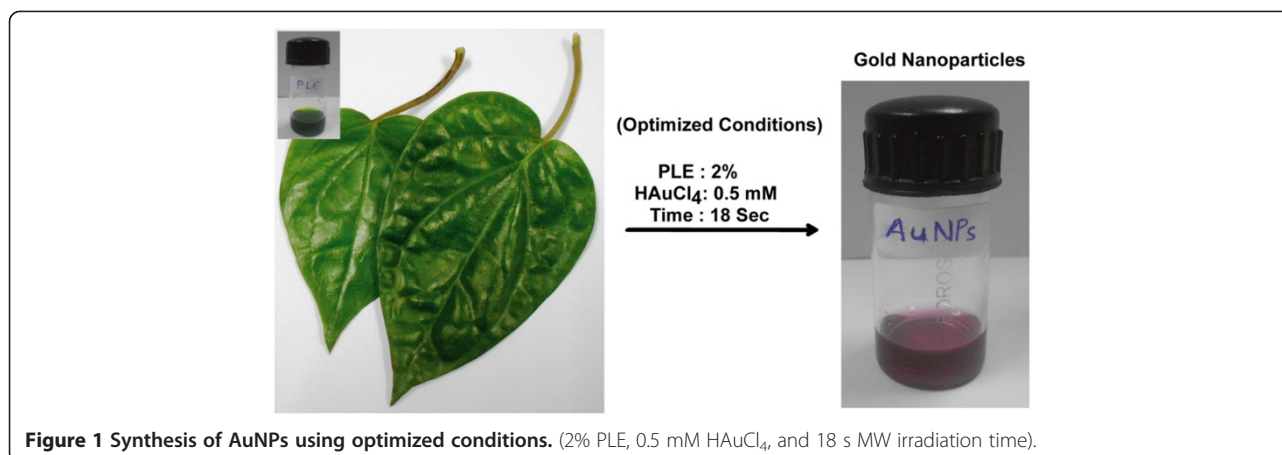
Figure 1 Synthesis of AuNPs using optimized conditions. (2% PLE, 0.5 mM HAuCl$_4$, and 18 s MW irradiation time).

Cytotoxicity studies

To maintain the HeLa (human cervical cancer) and MCF-7 (human breast cancer) cells, we used the minimal essential medium (MEM) containing 1.0 mM sodium pyruvate, 0.1 mM nonessential amino acids, 1.5 g/L sodium bicarbonate, 2 mM L-glutamine supplemented with 10% FBS (heat inactivated), and 1% antibiotic-antimycotic solution (1,000 U/mL penicillin G, 10 mg/mL streptomycin sulfate, 5 mg/mL gentamycin, and 25 μg/mL amphotericin B). The cells were cultured at 37°C in a humidified incubator (HF 160 W, Heal Force, Shanghai, China) supplemented with 5% CO$_2$.

To examine the cytotoxicity of AuNPs in cancer cells, monocultures of the HeLa and MCF-7 cell lines were incubated for 24 h with increasing concentrations of filter (0.2 micron)-sterilized AuNPs, and the cell viability

was estimated by MTT dye conversion assay. Cells not exposed to AuNPs were taken as control. Cells were seeded and maintained (1×10^4) in a 96-well plate (Cell Bind, Corning Inc., Corning, NY, USA) using MEM medium with serum. After 24 h of growth, the medium was replaced with the serum-free medium that contained varied concentrations of AuNPs (10 to 100 μM). The medium was removed after 24 h of treatment, and cells were washed with phosphate-buffered saline (0.01 M, pH 7.2). This was followed by the addition of 100 μl of MTT (0.5 mg/mL) prepared in serum-free medium to each well and incubation for 4 h at 37°C. After incubation, the medium was removed, and 100 μl of dimethyl sulfoxide (DMSO) was added to each well to solubilize the formazan crystals, and the concentration of formazan was determined by measuring its absorbance at 570 nm using
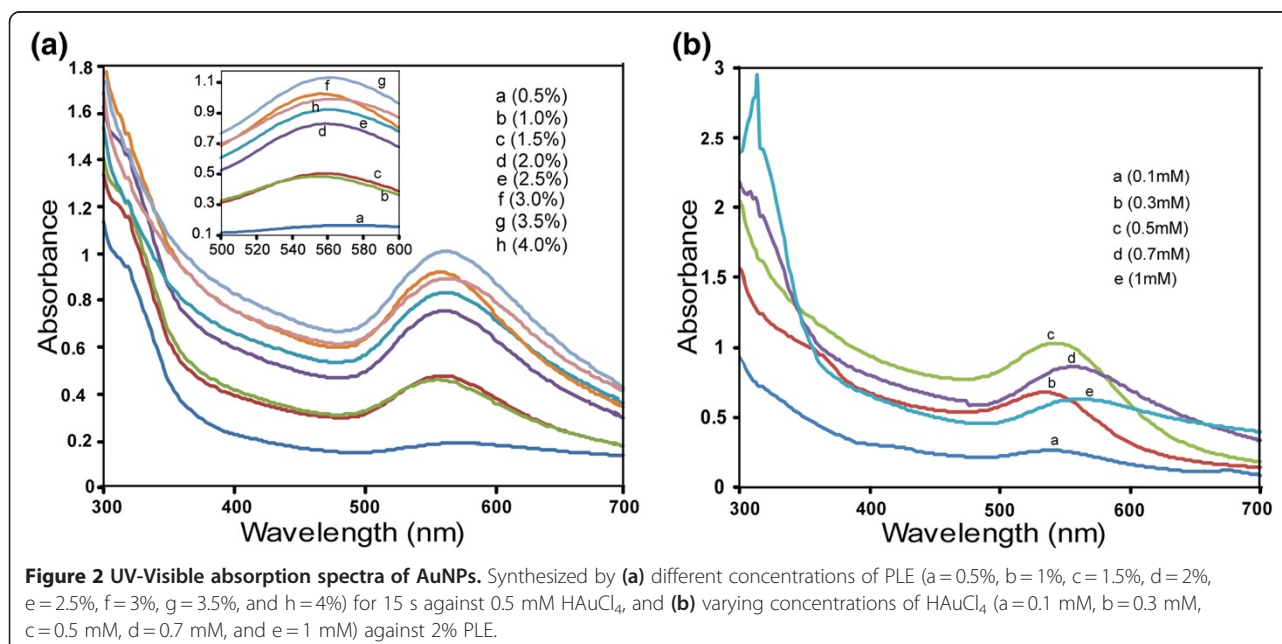

Figure 2 UV-Visible absorption spectra of AuNPs. Synthesized by **(a)** different concentrations of PLE (a = 0.5%, b = 1%, c = 1.5%, d = 2%, e = 2.5%, f = 3%, g = 3.5%, and h = 4%) for 15 s against 0.5 mM HAuCl$_4$, and **(b)** varying concentrations of HAuCl$_4$ (a = 0.1 mM, b = 0.3 mM, c = 0.5 mM, d = 0.7 mM, and e = 1 mM) against 2% PLE.

Table 1 UV-visible spectral analysis of the reaction mixtures and their λ_{max} peak positions

Number of runs	HAuCl$_4$ concentration (mM)	PLE extract (%)	MW irradiation time (s)	Observed λ_{max} peak position
1	0.5	0.50	15	538
2	0.5	1.00	15	534
3	0.5	1.50	15	530
4	0.5	2.00	15	544
5	0.5	2.50	15	550
6	0.5	3.00	15	558
7	0.5	3.50	15	548
8	0.5	4.00	15	548
9	0.1	2.00	15	544
10	0.3	2.00	15	542
11	0.5	2.00	15	547
12	0.7	2.00	15	558
13	1.0	2.00	15	564
14	0.5	2.00	12	550
15	0.5	2.00	14	552
16	0.5	2.00	16	550
17	0.5	2.00	18	556
18	0.5	2.00	20	552
19	0.5	2.00	22	554
20	0.5	2.00	24	552
21	0.5	2.00	26	548
22	0.5	2.00	28	548
23	0.5	2.00	30	548

PLE, *P. betle* leaf extract; MW, microwave irradiation.

a multiwell plate reader (Tecon micro plate reader, model 680, Tecon Inc., San Clemente, CA, USA). The cell viability was calculated with the following equation:

$$\text{Cell viability } (\%) = (A_{\text{treated}}/A_{\text{control}}) \times 100$$

where A_{treated} and A_{control} are the absorbances of the treated and untreated cells, respectively.

Results and discussion

Effect of PLE and HAuCl$_4$ on the AuNP synthesis

The formation of AuNPs was monitored with the naked eye by observing the appearance of the ruby red color, as shown in Figure 1. *P. betel* has a high content of phenolic acids, antioxidants, and flavonoids. The abundant hydroxyl groups available in these compounds could participate in the gold bioreduction. The bioreduction of gold could occur through the oxidation of hydroxyl (R–OH) to carbonyl groups (R–C = O), as shown in following equation:

$$AuCl_4^- + 3R - OH \rightarrow Au^o + 3R = O + 3H^+ + 4Cl^-$$
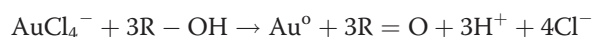
The SPR peak of 2% PLE against 0.5 mM gold solution showed intense and narrow peak centered around 544 nm, as shown in Figure 2a, whereas the SPR peaks above the 2% PLE concentration were flattening and red-shifted, indicating the formation of large-size AuNPs and those below the 2% concentration were considered as
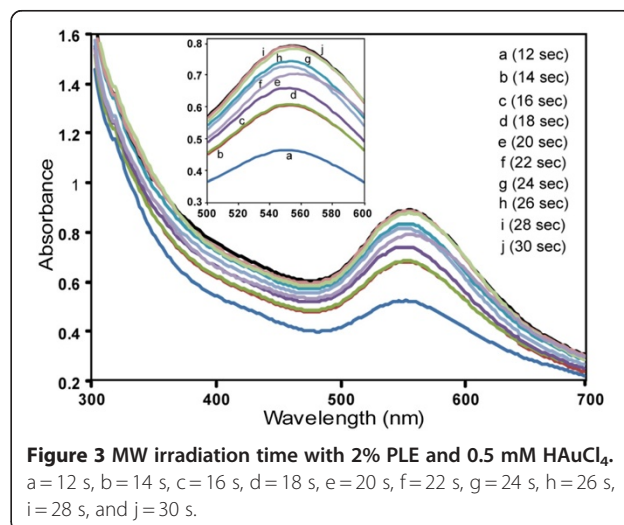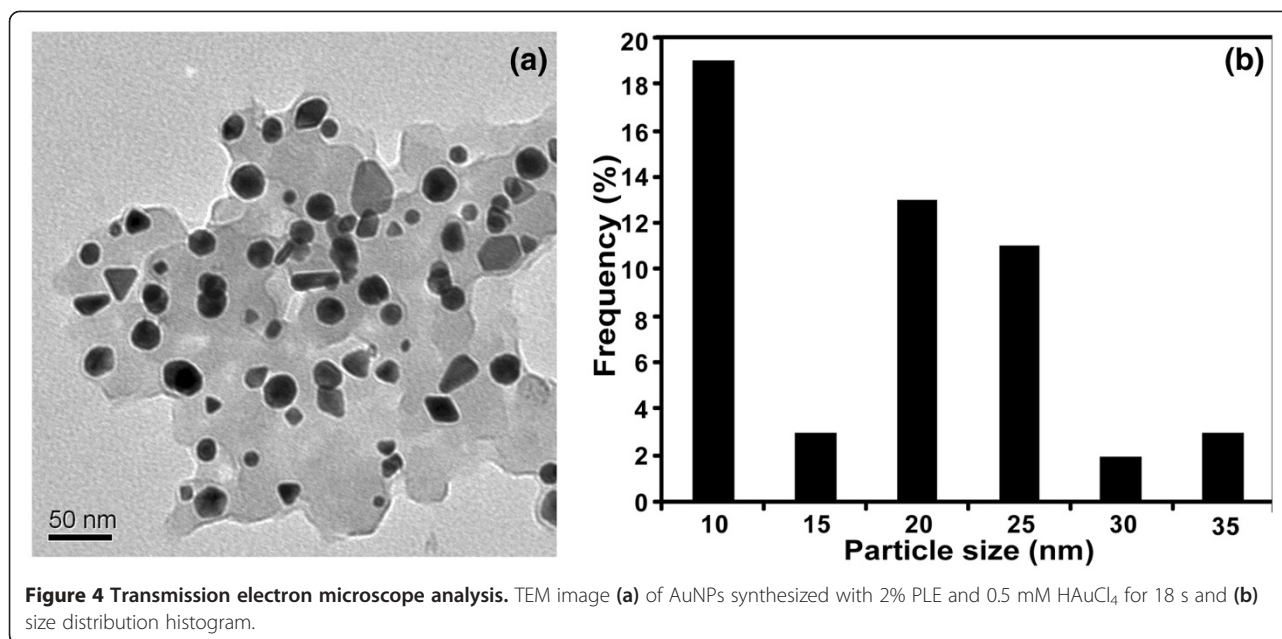

Figure 3 MW irradiation time with 2% PLE and 0.5 mM HAuCl$_4$.
a = 12 s, b = 14 s, c = 16 s, d = 18 s, e = 20 s, f = 22 s, g = 24 s, h = 26 s, i = 28 s, and j = 30 s.

Figure 4 Transmission electron microscope analysis. TEM image **(a)** of AuNPs synthesized with 2% PLE and 0.5 mM $HAuCl_4$ for 18 s and **(b)** size distribution histogram.
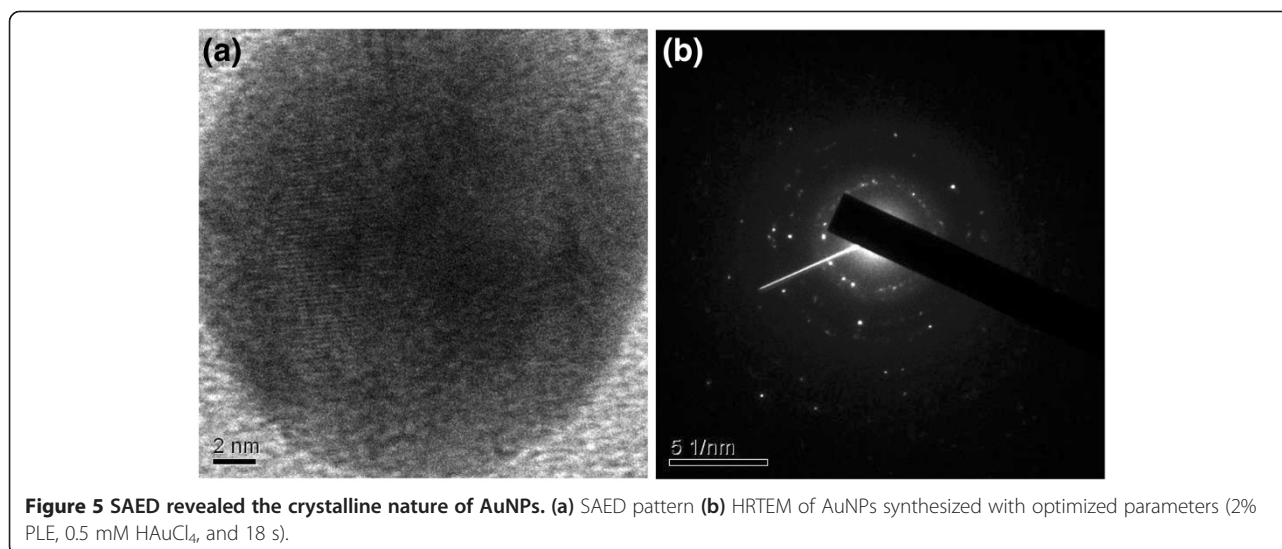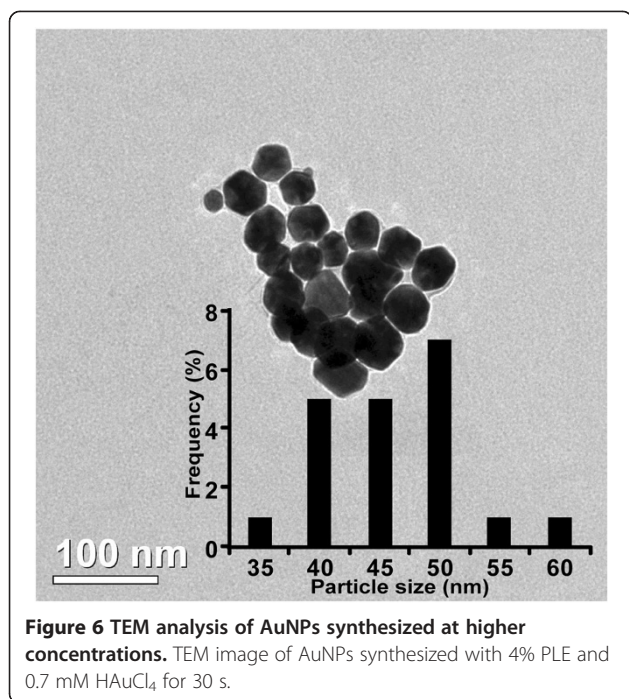
suboptimal. Thus, 2% PLE was considered as optimal for the synthesis of AuNPs. Figure 2b shows the UV–Vis spectra of products obtained by reacting 2% PLE with various concentrations of $HAuCl_4$ (0.1 to 1 mM), which displayed an intense peak at 547 nm for 0.5 mM $HAuCl_4$. However, the SPR peaks displayed by the 0.3 mM $HAuCl_4$ were suboptimal, whereas those of 0.7 and 1 mM $HAuCl_4$ were red-shifted. Since there was no significant formation of the peak with 0.1 mM, 0.5 mM $HAuCl_4$ was taken as the optimum for the synthesis of the AuNPs. UV-visible spectral analysis of the different reaction

products exhibited sharp SPR peaks presented in Table 1, indicating the successful formation of AuNPs.

Time-dependent synthesis of AuNPs
Figure 3 shows the various experiments carried out to determine the optimum time for the synthesis of AuNPs by incubating the 2% PLE and 0.5 mM gold solution at different time intervals (12 to 30 s) of microwave irradiation. We found that the peaks above 18 s were flattening, indicating no further significant formation of AuNPs. The peaks below 18 s were considered as suboptimal as they displayed poor intensity. This revealed

Figure 5 SAED revealed the crystalline nature of AuNPs. (a) SAED pattern **(b)** HRTEM of AuNPs synthesized with optimized parameters (2% PLE, 0.5 mM $HAuCl_4$, and 18 s).

Figure 6 TEM analysis of AuNPs synthesized at higher concentrations. TEM image of AuNPs synthesized with 4% PLE and 0.7 mM $HAuCl_4$ for 30 s.

Figure 8 FT-IR spectra of lyophilized PLE (spectrum a) and AuNPs (spectrum b).

that 18 s was sufficient to reduce the 0.5 mM gold solution to AuNPs, thereby proving it as optimum for the synthesis.

Synthesized AuNPs were characterized with various biophysical techniques

We have employed the TEM technique to visualize the size and shape of formed AuNPs. Figure 4a shows the typical bright-field TEM image of AuNPs obtained with optimum reaction conditions and reveals that the majority of AuNPs formed were circular in shape. The size of the synthesized AuNPs ranges from 10 to 35 nm, and the average size was found to be 6 nm, as shown in
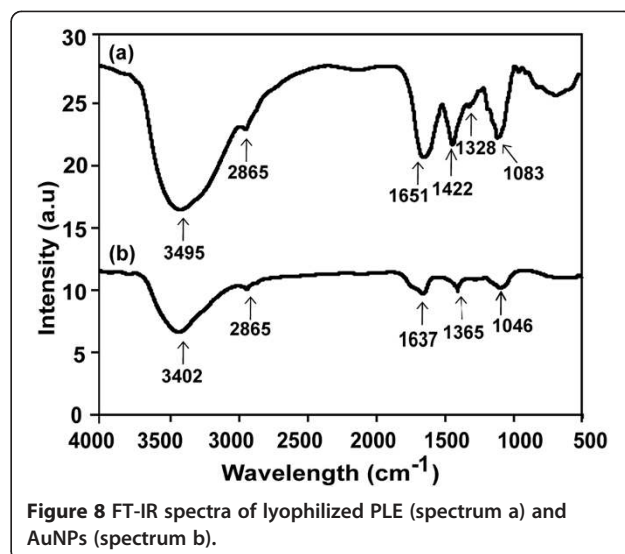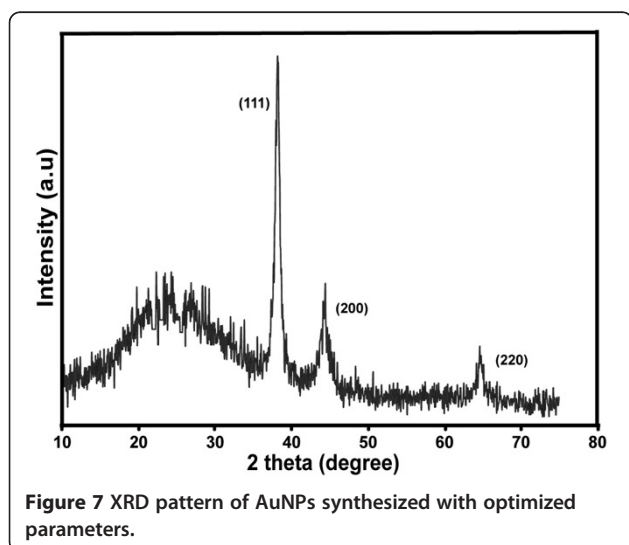
Figure 4b. Figure 5a shows the high-resolution TEM (HRTEM) image showing clear lattice fringes of 0.22 nm, revealing that the growth of the AuNPs occurred preferentially on the (1 1 1) plane. The interplaner distance of the Au (1 1 1) plane was in agreement with the (1 1 1) d-spacing of bulk Au (0.2355 nm) [23,24]. The crystalline nature of the synthesized AuNPs was confirmed from the selected area electron diffraction (SAED) pattern with bright circular rings corresponding to the (1 1 1), (2 0 0), and (2 2 0) planes, as shown in Figure 5b. [23,25]. Also, we observed the significant change in the peak position (red-shifted peaks) of the reaction mixture obtained by using 4% PLE and 0.7 mM $HAuCl_4$ for 30 s, indicating the formation of large-size AuNPs, which was confirmed using TEM technique. The TEM images shown in Figure 6 revealed the formation of large-size AuNPs, which agreed with the results obtained in Figure 2.
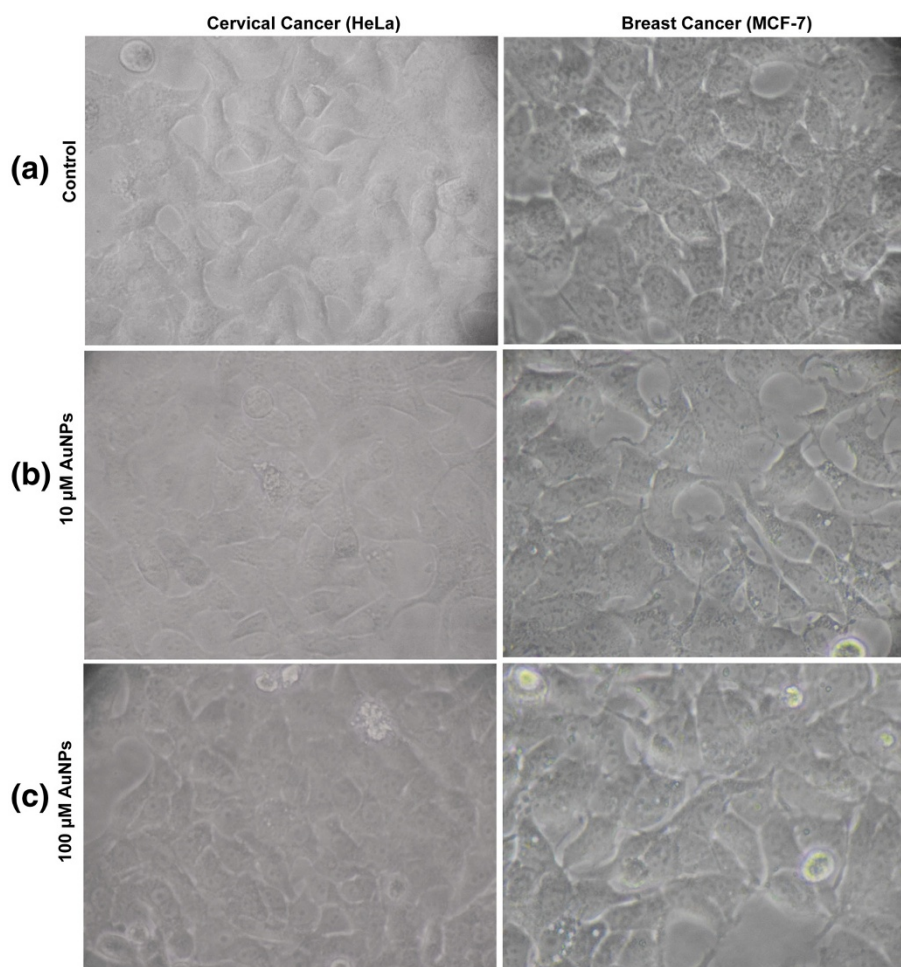

Figure 7 XRD pattern of AuNPs synthesized with optimized parameters.

Figure 9 EDX pattern. AuNPs synthesized with 2% PLE, 0.5 mM $HAuCl_4$, and 18 s MW irradiation time.
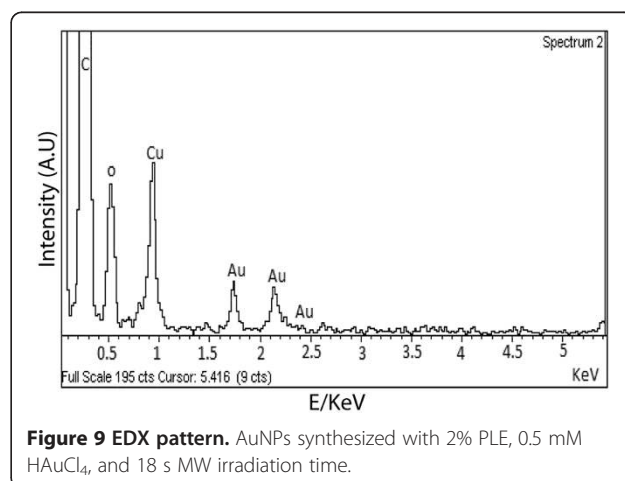
Figure 10 Images of cancer cell lines (HeLa and MCF-7). Over 24-h AuNP treatment; control, 10, and 100 μM.

Figure 7 shows the XRD (Bruker D8 ADVANCE X-ray powder diffractometer, Bruker AXS Inc, Madison, WI, USA) pattern of the AuNPs that showed three prominent Bragg reflections, which were indexed on the basis of the fcc structure of gold. The intensity of the (1 1 1), (2 0 0), and (2 2 0) diffraction peaks corresponding to 38.1°, 44.5°, and 64.8°, respectively, confirmed that the synthesized AuNPs were of crystalline nature [23,26,27].

Possibility of functional groups being involved in the synthesis of AuNPs

The involvement of functional groups in synthesized AuNPs was studied by FT-IR. The FT-IR spectra of PLE, as shown in Figure 8a, showed peaks at 3,495 cm^{-1} (hydroxyl group arising from alcohols and phenolic compounds), 2,865 cm^{-1} (secondary amine), 1,651 cm^{-1} (amide I bond of proteins), 1,422 cm^{-1} (C = C groups from alkenes), 1,328 cm^{-1} (C–CH$_3$ group), and 1,083 cm^{-1} (C–N stretching vibrations of amide bond), whereas the AuNPs showed peaks at 3,402, 2,865, 1,637, 1,365, and
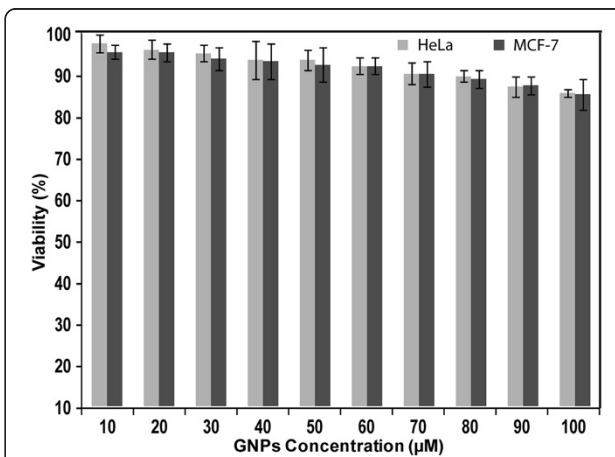
Figure 11 Cytotoxicity assay. Cell viability of HeLa and MCF-7 cells exposed to different concentrations of AuNPs (10 to 100 μM) over a 24-h treatment.

1,046 cm^{-1}, as indicated in Figure 8b [26,27]. The main significant difference between the spectrum of intact PLE before and after gold reduction is the disappearance peak at 1,328 cm^{-1} (curve a) and appropriate alteration of 1,422 to 1,365 cm^{-1}. This phenomenon revealed that biomolecules in the PLE, such as antioxidants, phenols, and flovonoids, that contain abundant aromatic C = C groups (1,422 cm^{-1}) may play an important role in the bioreduction and stabilization of AuNPs and may be responsible for the appearance of the significant peak at 1,365 cm^{-1} corresponding to the C–C bond. The three absorption peaks of AuNPs at 1,637, 2,865, and 3,042 cm^{-1} are attributed to the primary amines, alkyl, and OH groups, respectively. The reappearance of these groups in the spectrum of AuNPs suggested the attachment of some N–H, N = H, and OH groups onto AuNPs during the biosynthesis process. Hence, it was deduced that AuNPs might be capped and stabilized by biomolecules (antioxidants, flavonoids, and polyphenols) originating from PLE.

EDX analysis

Figure 9 shows the EDX profile of AuNPs, which revealed a strong signal for gold and Cu along with very strong carbon, nitrogen, and oxygen peaks. The signal for Cu originated from the grid used for the analysis. The resulting carbon and oxygen peaks may have originated from the antioxidants/flavonoids/phenolic or organic biomolecules bound to the surface of the AuNPs. The EDX and FT-IR together suggested the presence of biomolecules on the surface of the synthesized AuNPs.

PLE provided a nontoxic coating on the surface of AuNPs

The cytotoxicity of AuNPs under *in vitro* conditions in HeLa and MCF-7 cells was examined by MTT assay for 24 h in terms of effect of AuNPs on cell proliferation. Only cells that are viable after 24-h exposure to the AuNPs can metabolize MTT efficiently and produce purple colored crystal which is soluble in DMSO. Figure 10 shows unaltered cellular morphologies of two cell lines after treatment with AuNPs, suggesting that treatment with AuNPs did not induce any cytotoxic effect causing significant damage or death of the treated cells. Figure 11 shows the viability of both HeLa and MCF-7 cancer cell lines after 24 h post treatment and showed excellent viability as high as 100 μmol/L of AuNPs. This indicated that the PLE provided a nontoxic coating on the surface of AuNPs. This revealed that the synthesized AuNPs were of insignificant toxicity on cancer line, providing an opportunity for application in drug delivery and molecular imaging.

Conclusions

The method of AuNP synthesis described here has advantages such as rapidness, use of biologically benign biomaterial (PLE), and most importantly, resulting in biocompatible AuNPs. The synthesized AuNPs have insignificant toxicity at a maximum dose of 100 μM; thus, the particles could be very effective as a drug delivery tool and for other biomedical applications.

Author details
^{1}Biomaterials and Tissue Engineering Laboratory, Department of Biotechnology, Indian Institute of Technology Guwahati, Guwahati, Assam 781039, India. ^{2}Biotech Hub, Centre for the Environment, Indian Institute of Technology Guwahati, Guwahati, Assam 781039, India. ^{3}Department of Biotechnology, D.R.W. University, Gudur, SPS Nellore, Andhra Pradesh 524101, India.

References
1. J. Kasthuri, K. Kathiravan, N.J. Rajendiran, Phyllanthin-assisted biosynthesis of silver and gold nanoparticles: a novel biological approach. Nanopart. Res. **11**, 1075–1085 (2009)
2. M. Catherine, G. Man, D. Catherine, M. Cusker, Y. Tuna, V.M. Rotello, Toxicity of gold nanoparticles functionalized with cationic and anionic side chains. Bioconjugate Chem. **15**, 897–900 (2004)
3. S. Singh, H.S. Nalwa, Nanotechnology and health safety toxicity and risk assessments of nanostructured materials on human health. J Nanosci Nanotechnol **7**, 3048–3070 (2007)
4. V. Kattumuri, K. Katti, S. Bhaskaran, E.J. Boote, S.W. Casteel, G.M. Fent, Gum arabic as a phytochemical construct for the stabilization of gold nanoparticles: in vivo pharmacokinetics and X-ray-contrast-imaging studies. Small **3**, 333–341 (2007)
5. H. Gleiter, Nanostructured materials: basic concepts and microstructure. Acta Materialia. **48**, 1–29 (2000)
6. J.S. Bradley, G.E. Schmid, *Cluster and Colloids: From Theory to Application* (Wiley, Weinheim, 1994)
7. J.L. Elechiguerra, J.L. Burt, R.J. Morones, A. Camacho, X. Gao, H.H. Lara, Interaction of silver nanoparticles with HIV-1. J Nanobiotechnol. **3**, 1–10 (2005)
8. R. Niranjan, R. Nivedita, I. Ritu, S. Chandrasekaran, Phenolic antibacterials from *Piper betle* in the prevention of halitosis. J Ethnopharmacol **83**, 149–152 (2002)

9. F.A. Razak, R.Y. Othman, Z.H.A. Haji, Evaluation of antihistaminic activity of *Piper betel* leaf in guinea pig. J Oral Sci. **48**, 71–75 (2006)
10. G. Santhanam, S. Nagarjan, Development and validation of UV spectroscopic methods for the quick estimation of *Piper betle* leaf (PBL) extract. Fitoterapia **61**, 458–459 (1990)
11. M.S. Prabhu, K. Patel, G. Saraawathi, K. Srinivasan, Effect of orally administered betel leaf (*Piper betle* leaf Linn.) on digestive enzymes of pancreas and intestinal mucosa and on bile production in rats. Indian J Exp Biol **33**, 752–756 (1995)
12. N. Dasgupta, B. De, Antioxidant activity of Piper betel L. leaf extract in vitro. Food Chem **88**, 219–224 (2004)
13. D. Choudhury, R.K. Kale, Antioxidant and non-toxic properties of *Piper betle* leaf extract: in vitro and in vivo studies. Phytother Res. **16**, 461–466 (2002)
14. P. Tappayuthpijarn, Q. Dejatiwongse, P. Pongpech, A. Leelaporn, Antibacterial activity of extracts of *Piper betle* leaf. Thai J Pharmacol. **4**, 205–212 (1982)
15. L. Boonyaratanakornkit, P. Pothiyanont, N. Noppakun, P. Sinhaseni, A. Laorpaksa, S. Virunhaphol, Activity of betle leaf ointment on skin diseases. Thai J Pharm Sci. **15**, 277–287 (1990)
16. P. Pongpech, V.J. Prasertsilpe, The study of antimicrobial activity of *Piper betle* cream and gel against some fungi, yeast and bacteria. GPO. **19**, 8–22 (1993)
17. S. Bhattacharya, M. Subramanian, S. Roychowdhury, A.K. Bauri, J.P. Kamat, S.J. Chattopadhyay, Radioprotective property of the ethanolic extract of *Piper betel* leaf. Radiat Res **46**, 165–171 (2005)
18. L.S.R. Arambewela, L.D.A.M. Arawwawala, W.D. Ratnasooriya, Antidiabetic activities of aqueous and ethanolic extracts of *Piper betle* leaves in rats. J Ethnopharmacol **102**, 239–245 (2005)
19. Nanjing Zhongyiyao University, *The Dictionary of Traditional Chinese Medicines* (Shanghai Science and Technology Press, Shanghai, 2006)
20. P. Capdevielle-Pardies, J. David, J.L. Miquel, M. Le Bras, Quid of betel. Med Trop. **45**, 299–307 (1985)
21. K. Patel, S. Kapoor, D.P. Dave, Synthesis of nanosized silver colloids by microwave dielectric heating. J Chem Sci **117**, 53–60 (2005)
22. H.B. Yin, T. Yamamoto, Y.J. Wada, Large-scale and size-controlled synthesis of silver nanoparticles under microwave irradiation. Materials Chemi and Phys. **83**, 66–70 (2004)
23. S.S. Shankar, A. Rai, A. Ahmad, M. Sastry, Rapid synthesis of Au, Ag, and bimetallic Au core-Ag shell nanoparticles using Neem (*Azadirachta indica*) leaf broth. J Colloid Interface Sci **275**, 496–502 (2004)
24. P. Kannan, S.A. John, Synthesis of mercaptothiadiazole-functionalized gold nanoparticles and their self-assembly on Au substrates. Nanotechnology **19**, 085602 (2008)
25. S.S. Shankar, A. Rai, B. Ankamwar, A. Singh, A. Ahmad, M. Sastry, Biological synthesis of triangular gold nanoprisms. Nat Mater **3**, 482–489 (2004)
26. P.J. Babu, P. Sharma, M.C. Kalita, U. Bora, Green synthesis of biocompatible gold nanoparticles using *Fagopyrum esculentum* leaf extract. Front Mater Sci **5**, 379–387 (2011)
27. P.J. Babu, P. Sharma, B.B. Borthakur, R.K. Das, U. Bora, Synthesis of gold nanoparticles using *Mentha arvensis* leaf extract. International Journal of Green Nanotechnology: Physics and Chemistry **2**, 62–68 (2010)